Journal of Biomedical Optics

BiomedicalOptics.SPIEDigitalLibrary.org

Thermal evaluation of laser exposures in an *in vitro* retinal model by microthermal sensing

Tae Y. Choi
Michael L. Denton
Gary D. Noojin
Larry E. Estlack
Ramesh Shrestha
Benjamin A. Rockwell
Robert Thomas
Dongsik Kim

SPIE.

Thermal evaluation of laser exposures in an *in vitro* retinal model by microthermal sensing

Tae Y. Choi,[a,*] Michael L. Denton,[b] Gary D. Noojin,[b] Larry E. Estlack,[c] Ramesh Shrestha,[a] Benjamin A. Rockwell,[d] Robert Thomas,[d] and Dongsik Kim[e]

[a]University of North Texas, Department of Mechanical and Energy Engineering, 3940 N. Elm Street Denton, Texas 76207, United States
[b]TASC, Inc., Department of Biomedical Sciences and Technologies, 4141 Petroleum Road, JBSA Fort Sam Houston, Texas 78234, United States
[c]Conceptual MindWorks, Inc., 4141 Petroleum Road, JBSA Fort Sam Houston, Texas 78234, United States
[d]711th Human Performance Wing, Bioeffects Division, Optical Radiation Bioeffects Branch, 4141 Petroleum Road, JBSA Fort Sam Houston, Texas 78234, United States
[e]POSTECH, Department of Mechanical Engineering, San 31 Hyoja-Dong, Nam-Gu, Pohang, Gyungbuk 790-784, Republic of Korea

Abstract. A temperature detection system using a micropipette thermocouple sensor was developed for use within mammalian cells during laser exposure with an 8.6-μm beam at 532 nm. We have demonstrated the capability of measuring temperatures at a single-cell level in the microscale range by inserting micropipette-based thermal sensors of size ranging from 2 to 4 μm into the membrane of a live retinal pigment epithelium (RPE) cell subjected to a laser beam. We setup the treatment groups of 532-nm laser-irradiated single RPE cell and *in situ* temperature recordings were made over time. Thermal profiles are given for representative cells experiencing damage resulting from exposures of 0.2 to 2 s. The measured maximum temperature rise for each cell ranges from 39 to 73°C; the RPE cells showed a signature of death for all the cases reported herein. In order to check the cell viability, real-time fluorescence microscopy was used to identify the transition of pigmented RPE cells between viable and damaged states due to laser exposure. [DOI: 10.1117/1.JBO.19.9.097003]

Keywords: thermal sensing; retinal pigment epithelium; micropipette; laser.

Paper 140229R received Apr. 10, 2014; revised manuscript received Jul. 18, 2014; accepted for publication Aug. 25, 2014; published online Sep. 15, 2014.

1 Introduction

In order to study and model thermal responses of tissues to laser irradiation, temperature measurements must be made at the cellular level in real time with exposure. Conventional thermocouples are bulky and do not provide sufficient sensitivity for use in temperature measurements at the level of single cells. For example, line thermometers[1] are well suited to measure the temperature rise during laser irradiation, but spatial resolution suffers dramatically because measurement lines are 10-μm wide and 5-mm long. Originating from the work by Fish et al.,[2] an improved design of thermal microscale sensors was applied to the near-field scanning thermal microscope[3] to achieve high temporal (submicrosecond) and spatial responses. Another variation of a thermocouple-based sensor (with a spatial resolution of ~1 μm) was tested by Watanabe et al.,[4] although reliable application in living cells seems lacking. However, these previous works are involved with cost-ineffective manufacturing processes such as focused ion beam milling.[4] The sensor and sensor system developed in this work provide a cost-effective solution for microscale temperature measurement, which is based on a patented technology[5] and has been shown to enable various fields of biomedical research involved with cellular temperature change.

The importance of cellular level temperature sensing is emphasized in a wide range of fields including photothermal therapy, plasmonic heating of nanoparticles for cancer therapy,[6,7,8] and laser–tissue interaction.[9] Cellular level sensing of biological activities promises significant and broad impacts on many biological sciences as well as biomedical diagnosis. For example, the ability to measure the temperature in individual cells (or tissues) can provide important data on how drugs may affect brain hyperthermia.[10] Other important applications such as thermal therapy (cryotherapy),[11,12] metabolomic activity,[13] and heat-induced denaturation of DNA and proteins[14] need accurate, high-resolution temperature measurements. For example, the success of thawing and freezing individual cells (e.g., cancer cells) during cryotherapy for analysis relies on the accurate interpretation of temperature changes.

Alternatively, high-magnification infrared thermography has been used successfully in measuring temperature (8×8-μm effective pixel at sample) during laser exposure in an *in vitro* retinal model.[15,16] Here, the "microthermography" measurements were used to identify thermal thresholds for damage at the cellular level (8×8-μm effective pixel depth), whereas prior laser damage thresholds[17–19] were limited to laser irradiance or radiant exposure. However, as with any imaging system, multiple pixels are required for resolving power and the microthermography method is incapable of measuring the temperature responses of an individual cell. Herein, we demonstrate high-resolution temperature measurements for individual retinal pigment epithelium (RPE) cells during laser exposure *in vitro* using our novel micropipette system.

2 Experimental Details

The micropipette sensor used in this study was described elsewhere.[5,20] Briefly, the pulled pipette was filled with a lead-free soldering alloy mainly composed of tin (Sn) by an injection

*Address all correspondence to: T. Y. Choi, E-mail: choi@egw.unt.edu

0091-3286/2014/$25.00

molding process in conjunction with localized heating of material. The injection molding was accomplished by mechanical pressurization (pushing) of molten metal at the upper part of the pipette while heating the lower part near the tip with an electronic soldering gun maintained at 300°C. Then, a physical vapor deposition technique was used to coat thin films of nickel on the outer surface of the glass pipette, thus forming a Ni-Sn alloy contact at the sensor tip, which functions as a thermocouple junction. Based on the Seebeck coefficient difference of the two dissimilar metals used in this study, the sensor generates 7 to 15.5 μV/K. A prototype sensor [Fig. 1(a)] was fabricated according to the aforementioned procedures and tested in a calibration chamber. Reproducible calibration data at a resolution of ~10 mK were obtained.[20]

The uncertainty in the temperature measurement is associated with the resolution of the instrument (Kithley nanovoltmeter) and measurement error during calibration, which is determined statistically. The change in voltage signal due to temperature change in the surrounding fluid is converted into the temperature difference using the relationship $\Delta T = \Delta V/S$, where ΔT, ΔV, and S are the temperature difference, voltage difference, and Seebeck coefficient of the sensor, respectively. The root-sum-squared method is employed to estimate the error in the ΔT measurement.

$$u_{\Delta T} = \left[\left(\frac{\partial \Delta T}{\partial \Delta V} u_{\Delta V}\right)^2 + \left(\frac{\partial \Delta T}{\partial S} u_S\right)^2\right]^{1/2},$$

where $u_{\Delta V}$ and u_S are the resolution of the Kithley nanovoltmeter and the uncertainty in the Seebeck coefficient, respectively. The 73-nV resolution of the voltmeter and the ± 0.15 μV/K uncertainty in the Seebeck coefficient, both of which were determined by calibration, resulted in an error estimation of 3.7%.

Furthermore, there is a finite temperature difference between the sensor tip and the surrounding temperature. To quantify such a difference in order to evaluate the sensor accuracy for measurement of the true cell temperature, we used an IR camera (FLIR, Wilsonville, Oregon, ThermoVision SC6000) to acquire the steady-state local (~100-μm^2 region) temperature data of water into which a micropipette sensor was submerged and to compare the IR temperatures with those by the micropipette sensor. Figure 1(b) shows a representative thermal image of the pipette tip in the water bath to verify its location during measurements. For clarity, we include an additional image in air [Fig. 1(c)], which avoids the strong absorption of the light detected by the thermal camera (3 to 5 μm). During measurement, the temperature of the surrounding fluid was averaged over ~100 μm^2, where the spatial temperature deviation (<0.1°C) in the region of interest is much less than the specified accuracy of 1°C, which is estimated by the IR sensing system. A systematic difference in temperature of <0.3°C between the surrounding fluid (water) and the thermocouple has been identified in the temperature range between the room temperature (25°C) and 50°C. Therefore, the current micropipette sensor can measure the temperature of the cell with an accuracy of ~1°C.

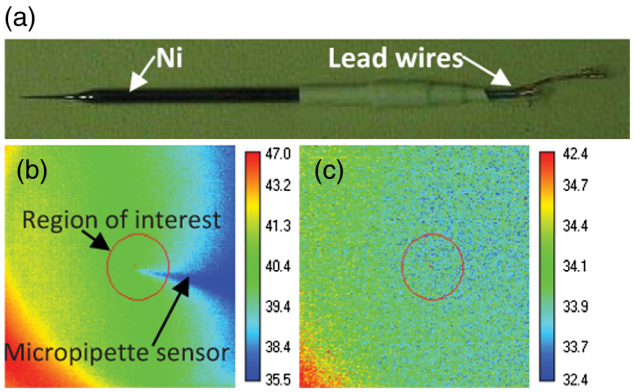

Fig. 1 (a) Prototype micropipette thermal sensor. Tin (Sn)-based alloy was filled by injection molding and the outer surface was coated with nickel (Ni) by sputtering. The contact made at the tip functions as a thermal sensor.[20] (b) Thermal image of heated water during calibration. The uniformity of temperature in the circled region of interest (c.a. 100 μm^2) where micropipette tip is expected to be is about ±0.1°C. (c) Thermal image of micropipette tip after removal of water (air is warmer).

Cell cultures of hTERT-RPE1, a human-derived RPE cell line (American Type Culture Collection, Manassas, Virginia), were grown and pigmented as described in our previous work.[19] Cells used in laser exposure experiments were seeded in 35-mm tissue culture dishes with glass bottom centers (MatTek Corporation, Ashland, Massachusetts) at 2×10^5 cells per plate. Four hours postseeding, the cells were artificially pigmented[19] with melanosome particles (MPs) at a concentration of 300 MPs/cell. The cell concentration was estimated using a known number of MPs based on the cell number and complete uptake was assumed during loading of MPs. At 24-h postseeding, the growth media were removed and the cells were washed twice with Hank's balanced salt solution (HBSS). Cells were preloaded with 4-μM calcein-AM (Invitrogen, Carlsbad, California) in HBSS for 10 to 20 min at 37°C. The calcein-AM solution was then removed and the cells were washed with HBSS to remove the residual dye. One milliliter of HBSS was then added to the cells for exposure to the laser.

3 Results and Discussion

At the time of laser exposure, a cell of interest was identified by the MP distribution around its nucleus using the bright-field portion of the in-house microscope shown in Fig. 2. Using computerized $x - y$ translational stages, the cell was positioned such that the 8.6-μm 532-nm laser beam was incident upon the cluster of MPs. Then, the micropipette was inserted into the cell until the tip was positioned about 5 μm from the nucleus. We have verified that the sensor tip was located inside the cell membrane by landing the tip on the glass substrate on which the RPE cells are attached and observing the cell image change. The cell image was observed to be distorted when the tip was inserted through the membrane. At least 10 min after inserting the micropipette, a prelaser dual bright-field and fluorescent image was taken to ensure the cell viability (calcein fluorescence) after manipulation. We used an excitation laser beam at 488 nm for taking the fluorescence image and focused around the nucleus with a size slightly smaller than the 532-nm heating laser; the heating laser will not quench the fluorescence of calcein-AM due to negligible absorption in the fluorescence particles. After laser exposure, a postlaser dual bright-field and fluorescent image provided evidence of cell damage (loss of fluorescence). Figure 3 provides data from a 200-ms laser exposure (2×10^4 J/cm^2). Notice the bright fluorescence in the nucleus of the target cell before the 532-nm laser was applied and how the fluorescence was eliminated postexposure in Fig. 3(b). The thermal profile recorded by the sensor tip conforms to the

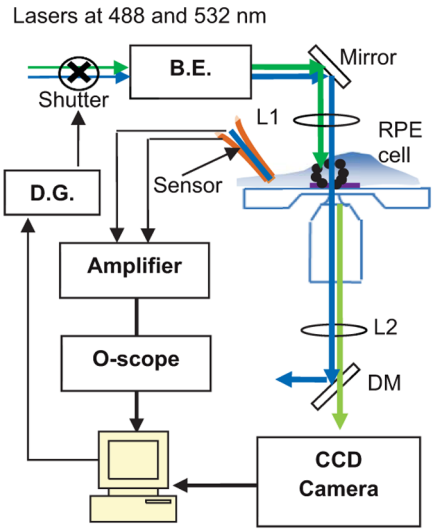

Fig. 2 Experimental setup. Incoming lasers are collinear. A dielectric mirror (not shown in the figure) highly reflective at 532 nm was used to direct both beams; most of 488-nm beam is transparent through this mirror. The two beams were expanded through a beam expander (B.E.). The generated thermopower was amplified and routed to oscilloscope (O-scope). The temperature data recording was made by LabVIEW. L1 is the focusing lens; L2 is the tube lens (at focal length of 400 nm); DM is the dichroic mirror (reflects 488 nm and transmits 515 nm) for fluorescence imaging; and D.G. is the delay generator.

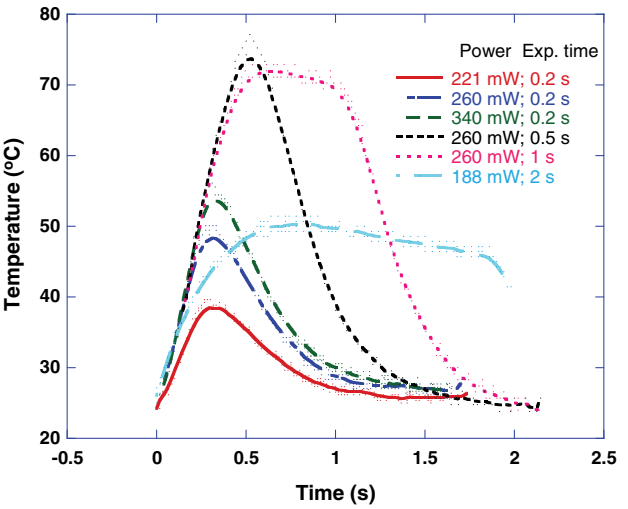

Fig. 4 Temperature profiles for additional damaging laser exposures. Representative thermal profiles are shown for laser exposure durations of 0.2 to 2 s and laser powers of 188 to 340 mW. All of these cases result in cell death.

expected temperature rise and decay appearance for a short laser exposure with moderate absorption. The peak temperature rise (55 ± 0.5°C) was well above the 10°C value commonly used to predict the cell death. Our temperature data demonstrate the feasibility of using the sensor to capture 532-nm laser-induced temperature changes in a single cell and confirms that these laser-induced temperature changes correlated with cell death. As control experiments, temperature recordings without pigments and without laser were also made and are indicated in Fig. 3(a). It should be noted that the spatial resolution of temperature can be estimated at 2 μm, which is based on the sensor tip diameter; a supporting image indicating the size of the tip is shown in Fig. 3(b).

The tip temperature increased without the presence of pigments because of the absorption of laser light from the spatial Gaussian tail of the laser exposure beam to the thermocouple tip. The temperature rise in this case turned out to be about one third of the pigmented cell temperature rise [Fig. 3(a)]. This will have a negligible effect on the cellular temperature rise because of the ultrasmall size of the sensor tip (corresponding tip to cell volume ratio of $\sim 1:100$).

We expect that there is an insignificant temperature difference ($\ll 1$°C) between the tip of the sensor and the laser spot because the RPE cell can be treated as a lumped system. In the current study, Biot number (Bi), an indicator to show the validity of using a lumped system, is much less than 1, which implies that the conduction heat transfer is much greater than the convection heat transfer. Bi is calculated as $\mathrm{Bi} = hL_c/k$, where h is the convective heat transfer coefficient (for natural convection, $h \sim 10$ W/m^{2}K), L_c is the cell dimension (up to 20 μm), and k is the thermal conductivity of the cell, which is close to that of water, 0.61 W/mK. Therefore, at the given spatial dimension (~ 20 μm), the temperature of the cell in the laser spot should be close to that at the sensor location.

Figure 4 shows the thermal profiles recorded during additional damaging laser exposure of individual RPE cells at various laser powers and exposure durations. In each case, the peak temperature within the recorded thermal profile matched both the exposure duration and indicated temperature rises of at

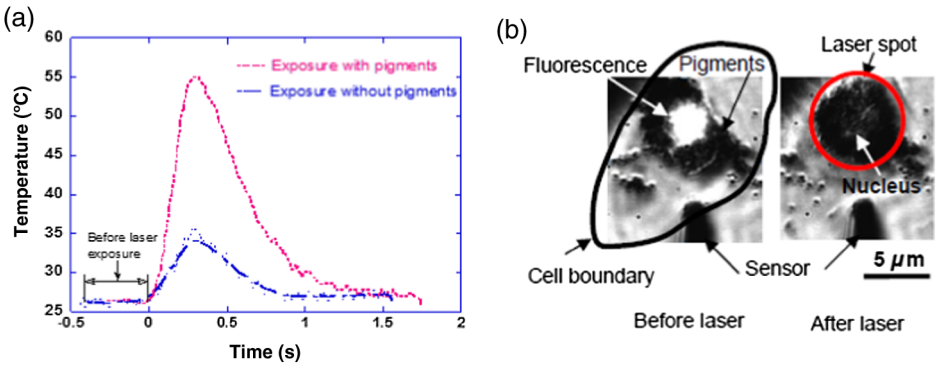

Fig. 3 Microthermometry from within an RPE cell. A single 200-ms laser pulse at 532 nm and fluence of 2×10^4 J/cm^2 was irradiated on the pigments accumulated around nucleus. (a) Temperature measurements were made in real time using the micropipette sensor (tip shown in inset image), and the resulting thermal profile is provided. Notice the loss of the bright calcein fluorescence in the nucleus as the result of the laser exposure indicating cellular damage in (b).

least 10°C. The data for the 0.2-s exposure at 221 mW indicated an approximate temperature rise of 15°C, but due to the fact that our data were collected at room temperature (25°C), the absolute temperature was measured to be 39 ± 0.5°C. This peak temperature leading to cell death seems low in our experience, especially considering that the exposure was only 0.2 s. This may be due to several causes relating to the complexity of the experiment. Positioning the micropipette tip to exactly 5 μm radially from the exposure site is difficult and it is always possible that the tip was out of plane axially (z-dimension) to some extent ($\sim$1 μm from the glass substrate). Additionally, the number of MPs within the exposure site varied from cell to cell because of nonuniform intracellular distribution and this would lead to differences in the extent of heating by the same laser power. The correlation between the MPs concentration versus temperature rise during laser illumination is currently under investigation.

4 Conclusion

In conclusion, we have developed a novel technique that measures microscale temperature increases in individual RPE cells at a spatial resolution of $\sim$2 μm. Measurements were made using a micropipette thermal sensor that was inserted into a living cell. *In situ* fluorescence images before and after laser exposure indicated cell death for comparisons with the recorded thermal profiles. This temperature measurement technique provides a fundamental advancement in the field of laser bioeffects.

Acknowledgments

This work was sponsored by an ASEE summer faculty fellowship from the U.S. Air Force Research Laboratory, the 711th Human Effectiveness Directorate. Support to MLD, GDN, and LEE was in the form of AFRL contract FA8650-08-D-6920. This work was partially supported by IT Consilience Creative Program of MKE and NIPA (C1515-1121-0003).

References

1. F. Ladieu, P. Martin, and S. Guizard, "Measuring thermal effects in femtosecond laser-induced breakdown of dielectrics," *Appl. Phys. Lett.* **81**(6), 957–959 (2002).
2. G. Fish et al., "Ultrafast response micropipette-based submicrometer thermocouple," *Rev. Sci. Instrum.* **66**(5), 3300–3306 (1995).
3. U. F. Wischnath et al., "The near-field scanning thermal microscope," *Rev. Sci. Instrum.* **79**, 073708 (2008).
4. M. S. Watanabe et al., "Micro-thermocouple probe for measurement of cellular thermal responses," in *Proc. IEEE, Engineering in Medicine and Biology 27th Annual Conf.*, IEEE (2005).
5. T. Y. Choi, "Multifunctional micropipette biological sensor," U.S. Patent 8,602,644 (2013).
6. X. Huang et al., "Determination of the minimum temperature required for selective photothermal destruction of cancer cells with the use of immunotargeted gold nanoparticles," *Photochem. Photobiol.* **82**(2), 412–417 (2006).
7. C. Loo et al., "Immunotargeted nanoshells for integrated cancer imaging and therapy," *Nano Lett.* **5**(4), 709–711 (2005).
8. V. P. Zharov et al., "Synergistic enhancement of selective nanophotothermolysis with gold nanoclusters: potential for cancer therapy," *Lasers Med. Surg.* **37**(2), 219–226 (2005).
9. A. Vogel and V. Venugopalan, "Mechanisms of pulsed laser ablation of biological tissues," *Chem. Rev.* **103**(2), 577–644 (2003).
10. E. A. Kiyatkin, "Brain hyperthermia as physiological and pathological phenomena," *Brain Res. Rev.* **50**(1), 27–56 (2005).
11. G. V. Gavriloaia et al., "Multimodal biomedical imaging IV," *Proc. SPIE* **7171**, 71710W (2009).
12. J. K. Seifert, T. Junginger, and D. L. Morris, "A collective review of the world literature on hepatic cryotherapy," *J. R. Coll. Surg. Edinburgh* **43**(3), 141–154 (1998).
13. D. E. Blask et al., "Melatonin inhibition of cancer growth in vivo involves suppression of tumor fatty acid metabolism via melatonin receptor-mediated signal transduction events," *Cancer Res.* **59**(18), 4693–4701 (1999).
14. M. Mandel et al., "Correlation of melting temperature and cesium chloride buoyant density of bacterial deoxyribonucleic acid," *J. Bacteriol.* **101**(2), 333–338 (1970).
15. M. L. Denton et al., "Determination of threshold average temperature for cell death in an in vitro retinal model using thermography," *Proc. SPIE* **7175**, 71750G (2009).
16. M. L. Denton et al., "Spatially correlated microthermography maps threshold temperature in laser-induced damage," *J. Biomed. Opt.* **16**(3), 036003 (2011).
17. M. L. Denton et al., "Damage thresholds for exposure to NIR and blue lasers in an in vitro RPE cell system," *Invest. Ophthalmol. Visual Sci.* **47**(7), 3065–3073 (2006).
18. M. L. Denton et al., "Damage thresholds for cultured retinal pigment epithelial cells exposed to lasers at 532 nm and 458 nm," *J. Biomed. Opt.* **12**, 034030 (2007).
19. M. L. Denton et al., "An in vitro model that approximates retinal damage threshold trends," *J. Biomed. Opt.* **13**(5), 054014 (2008).
20. R. Shrestha et al., "High-precision micropipette sensor for cellular-level real-time thermal characterization," *Sensors* **11**, 8826–8835 (2011).

Biographies of the authors are not available.